



Full Length Article

Green synthesis, characterization and antimicrobial activity of iron oxide nanoparticles with tigecycline against multidrug resistant bacterial strains

Mohamed Taha Yassin^{*}, Fatimah O. Al-Otibi, Abdulaziz A. Al-Askar

Botany and Microbiology Department, College of Science, King Saud University, P.O. 2455, Riyadh 11451, Saudi Arabia

ARTICLE INFO

Keywords:

Green synthesis
Iron oxide nanoparticles
Characterization
Antibacterial efficiency
Tigecycline
Synergism

ABSTRACT

Objectives: The current study focused on the green synthesis of iron oxide nanoparticles (IONPs) using *Salvia officinalis* leaf extract, aiming to control nosocomial infections caused by drug-resistant bacterial pathogens. The nanoparticles were characterized and evaluated for antibacterial effectiveness.

Methods: The disc diffusion assay was utilized to determine the synergistic antibacterial efficiency of the biogenic IONPs against three nosocomial bacterial pathogens namely, methicillin-resistant *Staphylococcus aureus* (MRSA), *Escherichia coli* and *Pseudomonas aeruginosa* strains.

Results and conclusion: The change of color of ferric nitrate solution from orange to black color after addition of the extract preliminary indicated the formation of biogenic IONPs. The phytosynthesized IONPs were characterized using UV-Vis spectroscopy indicating the formation of a broad band at 349 nm. Moreover, X-ray powder diffraction (XRD) analysis revealed the formation of diffraction peaks positioned at 2 theta degrees of 24.80°, 33.41°, 35.03°, 41.28°, 49.15°, 53.41°, 57.37°, 62.40° and 64.31°, corresponding to lattice planes of (012), (104), (110), (202), (024), (116), (214) and (300), respectively. The phytosynthesized nanoparticles revealed a high antibacterial activity against the concerned pathogens at the concentration of 200 µg/disc with relative inhibitory zones of 21.14 ± 0.16, 17.26 ± 0.26, and 20.56 ± 0.62 mm, respectively against *E. coli*, *P. aeruginosa* and MRSA strains. The biogenic IONPs revealed the highest synergistic activity with tigecycline antibiotic against *E. coli* followed by MRSA and *P. aeruginosa* strains with relative increase in fold of inhibition values (IFA) of 1.79, 1.29 and 0.93, respectively. In conclusion, the water extract of *S. officinalis* facilitated the green fabrication of IONPs with distinctive physicochemical properties and synergistic antibacterial activity against the tested nosocomial bacterial pathogens.

1. Introduction

Antimicrobial resistance is a significant public health issue, causing 1.27 million deaths worldwide and an estimated 5 million fatalities in 2019. In the United States, over 2.8 million illnesses exhibit antibiotic resistance, with the number of fatalities exceeding 35,000 individuals (Hetta et al., 2023). Resistant strains of *Escherichia coli* are a significant contributor to bloodstream and urinary tract infections (UTI) in both community and healthcare settings (Mills et al., 2022). Sepsis is a prevalent manifestation of urinary tract infections caused by *E. coli*. *Pseudomonas aeruginosa* is an opportunistic human pathogen that can cause severe respiratory infections in individuals with compromised

immune systems. It is the causative agent of 10 % of nosocomial infections and is prevalent in healthcare facilities, particularly in cases involving chronic wounds, urinary tract devices, or respiratory support (De Oliveira et al., 2020). Methicillin-resistant *Staphylococcus aureus* (MRSA) causes over 20 % of bloodstream infections, with overall mortality ranging from 15 to 50 %. These bacterial strains pose significant threats to public health and public health (Kaasch et al., 2014).

Iron oxide nanoparticles (IONPs) are a significant scientific and technological advancement due to their potential applications in gas sensors, catalysis, biosensing, water remediation, high-density magnetic recording media, targeted drug delivery, and cancer treatment (Sajid and Plotka-Wasylika, 2020). The chemical synthesis of IONPs has

Abbreviations: MIC, Minimum inhibitory concentration; MBC, Minimum bactericidal concentration; MHA, Mueller-Hinton agar; IONPs, Iron oxide nanoparticles; TGC, Tigecycline; XRD, X-ray Powder Diffraction.

Peer review under responsibility of King Saud University.

^{*} Corresponding author at: Botany and Microbiology Dept., College of Science, King Saud University, P. O. Box 2455, Riyadh 11451, Saudi Arabia.

E-mail address: myassin2.c@ksu.edu.sa (M. Taha Yassin).

<https://doi.org/10.1016/j.jksus.2024.103131>

Received 8 July 2023; Received in revised form 3 February 2024; Accepted 5 February 2024

Available online 8 February 2024

1018-3647/© 2024 The Author(s). Published by Elsevier B.V. on behalf of King Saud University. This is an open access article under the CC BY-NC-ND license (<http://creativecommons.org/licenses/by-nc-nd/4.0/>).

potential environmental drawbacks, such as the use of toxic solvents and energy consumption (Duan et al., 2015). A green chemistry approach has been introduced to synthesize IONPs using plant extracts, which include biomolecules like enzymes, vitamins, proteins, amino acids, phenolic compounds, and polysaccharides (Al-Otibi et al., 2023). There have been reports documenting the utilization of leaf extracts from various plant species, including *Sida cordifolia* (Pallela et al., 2019), *Zea mays* (Patra et al., 2017), *Couroupita guianensis* (Sathishkumar et al., 2018), *Argemone mexicana* (Arokiyaraj et al., 2013), and *Cynometra ramiflora* (Groiss et al., 2017). The IONPs have shown antibacterial effectiveness at concentrations ranging from 10 to 20 mg/mL (Shkodenko et al., 2020). The growth of *E. coli*, *Salmonella* Typhimurium, *Klebsiella pneumoniae*, and *Staphylococcus aureus* was inhibited by the biogenic Fe₃O₄ nanoparticles synthesized using *Couroupita guianensis* extract (Sathishkumar et al., 2018). *Salvia officinalis* L., a member of the Lamiaceae family, has potential therapeutic attributes, including antibacterial, antifungal, antioxidant, antiviral, and anticancer effects. The antimicrobial efficiency of the extract derived from *S. officinalis* leaves underscores its potential use in producing bioactive nanoparticles (Miraj and Kiani 2016). The prevalence of nosocomial infections caused by drug-resistant bacterial strains highlights the need for novel antimicrobial medicines to combat these infections in healthcare settings. This study aimed to environmentally synthesize IONPs using an aqueous leaf extract of *S. officinalis*. The nanoparticles were characterized using various physicochemical techniques, and their antibacterial efficacy against three nosocomial bacterial strains was evaluated.

2. Materials and methods

2.1. Preparation of plant extract

The *S. officinalis* dried leaves were procured at a local market located in Riyadh, Saudi Arabia. The verification of plant samples' identity was conducted by the herbarium affiliated with the department of Botany and Microbiology. The dried leaves of *S. officinalis* underwent a triple cleaning method, which including the use of distilled water after an initial wash with tap water. Subsequently, the desiccated leaves were subjected to natural air drying in the surrounding environment. The leaves underwent a process of pulverization, resulting in the production of a finely powdered substance with a consistent texture, achieved by the use of a mechanical blender. A flask with a capacity of 500 ml was used to accommodate a quantity of 50 g of plant powder together with 200 ml of distilled water. The flask was exposed to a temperature of 60 °C for a period of 30 min using a hot plate. The flask was thereafter subjected to continuous agitation for a period of 24 h at a temperature of 25 °C using a magnetic stirrer. Subsequently, the combination was subjected to filtration using Whatman filter paper (1) to acquire a pure filtrate and eliminate any residual contaminants. Following that, the extract was subjected to sterilization through filtering with a 0.45 µm Millipore membrane filter. Following this, the produced extracts were stored at a temperature of 4 °C for future research.

2.2. Biosynthesis of Fe₂O₃ nanoparticles

Ferric nitrate (Fe(NO₃)₃·9H₂O) of purity ≥ 98 % was purchased from Sigma Aldrich, U.K. For synthesis of IONPs, 0.01 M Ferric nitrate (Fe(NO₃)₃·9H₂O) solution will be added to the prepared aqueous extract of *S. officinalis* in a 1:1 proportion. The concentration of the plant extract was 7.8 g/L and the reaction was done under room temperature (25 °C ± 2). Formation of black color indicated the formation of IONPs. The reduced solution was centrifuged at 10,000 rpm for 10 min and supernatant was discarded. The pellets were washed thrice with distilled water for removal of impurities. Finally, the biogenic IONPs were dried in an oven at 32 °C, yielding a black powder and the reaction yield was detected to be 9.33 mg/ml. The pH of the reaction was monitored and seen to rise from an initial value of 1.98, corresponding to the pH of the

ferric nitrate solution, to a final value of 5.56, representing the pH of the reaction mixture at the end of the reaction and after addition of plant extract. According to a recent study by Akintelu et al. (2021), it was found that the synthesis of IONPs using plant extract is not favored under extreme acidic and basic conditions. In this context, it was observed that the addition of plant extract to the reaction mixture resulted in an increase in pH value, which potentially stimulated the formation of biogenic IONPs.

2.3. Physicochemical characterization of the biogenic IONPs

Different methods were used to analyze the biogenic IONPs, including UV-Vis spectroscopy, which was used to assess the optical characteristics of the IONPs. The morphology and size distribution of the biologically synthesized iron oxide nanoparticles (IONPs) were analyzed using a Transmission Electron Microscope (TEM) (model JEM1011, JEOL, Tokyo, Japan). In addition, the elemental composition of IONPs was evaluated using Energy-Dispersive X-ray (EDX) analysis. In addition, a Fourier transform infrared spectroscopy (FTIR) study was used to identify the main functional groups found in the biofabricated IONPs. The biogenic iron oxide nanoparticles (IONPs) were subjected to X-ray powder diffraction (XRD) analysis to confirm their crystalline structure and determine their crystal size. The Zeta sizer equipment (Malvern Instruments Ltd; zS90, Worcestershire, UK) was used to evaluate the zeta potential value and hydrodynamic diameter of IONPs.

2.4. Evaluation of antibacterial efficiency of the biosynthesized IONPs

The susceptibility of three nosocomial microbial strains, namely methicillin-resistant *Staphylococcus aureus* (ATCC 43300), *Escherichia coli* (ATCC 25922), and *Pseudomonas aeruginosa* (ATCC 9027) to the biogenic IONPs was investigated. *P. aeruginosa* (ATCC 9027) and MRSA (ATCC 43300) strains were reported as MDR pathogens in a previous study (Yassin et al., 2022). The bacterial suspension was prepared by utilizing a sterile saline solution with a concentration of 0.85 %. This was achieved by selecting fresh colonies from 24-hour cultures and immersing them into the saline solution. To achieve viable bacterial cell count of 1.0×10^8 , the turbidity of the microbial suspension was adjusted using a 0.5 McFarland standard. The bacterial suspension (0.5 mL) was transferred and evenly distributed onto freshly prepared Mueller-Hinton agar (MHA) medium. Tigecycline, which was used as standard antibacterial agent, was acquired from Sigma-Aldrich (St. Louis, MO, USA). Subsequently, sterile filter paper discs (8 mm in diameter) were impregnated with tigecycline to attain final concentration of 15 µg/disk, serving as positive controls. Furthermore, 8 mm diameter sterile filter paper discs were impregnated with 100 and 200 µg of the biosynthesized IONPs following their dispersion in methanol solvent. Filter paper discs saturated with methanol alone were employed as negative controls. Subsequently, the loaded discs were positioned on top of the seeded layer of MHA plates. Following this, the plates were refrigerated for 4 h to facilitate the diffusion of the biogenic IONPs through the medium. The measurement of inhibition zones was conducted using a Vernier caliper following a 24-hour incubation period at 35 °C. The broth microdilution assay was employed to determine the minimum inhibitory concentration of the biogenic IONPs produced from the leaf extract of *S. officinalis*. Furthermore, the determination of the minimum bactericidal concentration (MBC) was conducted by culturing the inoculums obtained from wells with minimum inhibitory concentration (MIC) over freshly prepared Mueller-Hinton agar (MHA) plates. These plates were then incubated at a temperature of 35 °C for a period of overnight incubation. Finally, the plates were examined to assess the presence or absence of bacterial growth. The minimum concentration of biogenic IONPs at which no bacterial growth was observed were recorded as MBC.

2.5. Determination of synergistic patterns of the biogenic IONPs with tigecycline

The standard disc diffusion method was employed to assess the combined antibacterial efficacy of biogenic IONPs (200 µg/disk) and tigecycline antibiotic (15 µg/disk) in a synergistic manner. The sterile filter paper discs, measuring 8 mm in diameter, were loaded with 200 µg of IONPs. In another group, the discs were impregnated with both the tigecycline antibiotic and IONPs. Furthermore, the experimental setup involved the loading of control discs with tigecycline antibiotic and methanol solvent, representing the positive and negative controls, respectively. Subsequently, the loaded discs were positioned onto the seeded layer of MHA plates, following the previously outlined procedure. Subsequently, the percentage of synergism (%) was calculated using the equation provided below:

$$\text{Synergism}(\%) = (B - A)/A \times 100$$

Whereas, A: referred to the inhibition zone diameter of tigecycline antibiotic and B: referred to the inhibition zone diameter of the combined tigecycline and the biogenic IONPs.

The increase in fold of inhibition area (IFA) value was calculated according to the following formula: $(\text{IFA}) = (B^2 - A^2)/A^2$, whereas A: referred to the inhibition zone diameter of tigecycline antibiotic and B: referred to the inhibition zone diameter of the combined tigecycline and the biogenic IONPs.

2.6. Statistical analysis

The study data were subjected to statistical analysis using GraphPad Prism version 8.0 (GraphPad Software, Inc., La Jolla, CA, USA) through the application of the Tukey test in a One-way ANOVA with a significance level of 0.05. The experiments were conducted in triplicate, and the resulting data were reported as the mean of triplicate measurements \pm the standard error. The particle size distribution histogram, FTIR and XRD pattern were generated using OriginPro 2018 software.

3. Results

3.1. Green synthesis of IONPs

The water extract of *S. officinalis* leaves was utilized for the green synthesis of IONPs as seen in Fig. 1a. The plant extract of *S. officinalis* act as a reducing agent of ferric nitrate solution resulting in formation of IONPs.

3.2. UV spectral analysis

UV-Vis spectral analysis of the biosynthesized IONPs revealed the presence of two absorption peaks at 244 and 349 nm (Fig. 1b). However, UV-analysis of the plant extract affirmed the formation of UV absorption band at 242 nm. The band noticed at λ_{max} around 200 could be assigned to adsorption of phytochemical constituents as flavonoids, polyphenolic compounds, and heteroatoms as N, S, O and unsaturated groups. Taken together, the absorption peak found at 349 nm could be assigned to the surface plasmon resonance of biogenic IONPs.

3.3. TEM analysis of the biofabricated IONPs

TEM analysis was conducted to estimate the shape and size of the phyto-synthesized IONPs. In this context, the average particle size was detected to be 42.327 nm (Fig. 2a). Moreover, TEM micrographs revealed that the nanoparticles exhibit a spherical morphology, with certain particles exhibiting agglomeration. Particle size distribution histogram indicated that the size of the phyto-synthesized IONPs ranged from 10 to 80 nm in diameter with average particle size of 42.327 nm

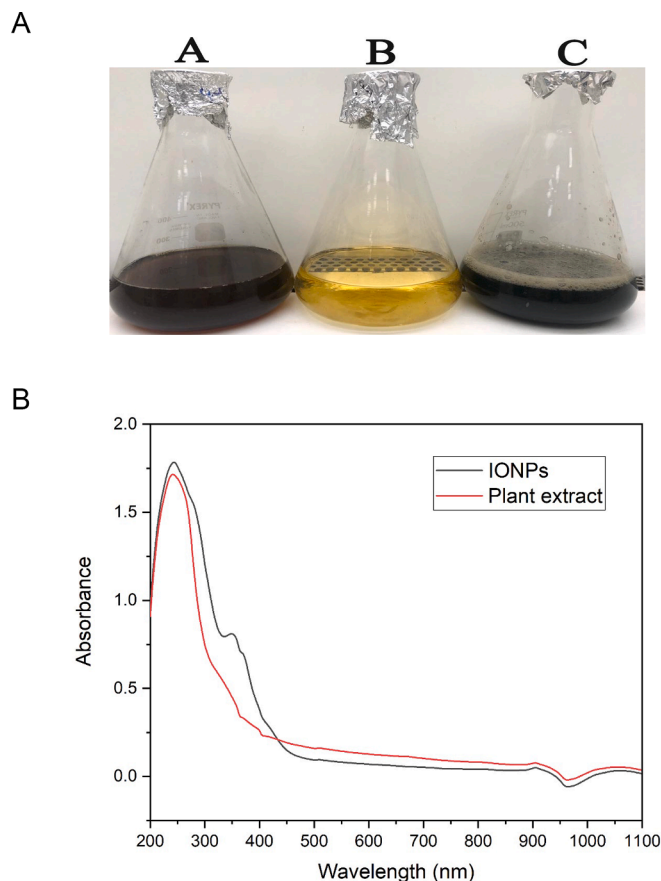


Fig. 1. a. Green biofabrication of IONPs using *S. officinalis* extract. (A): Water extract of *S. officinalis*, (B): Ferric nitrate solution, (C): IONPs; **Fig. 1b.** UV-Vis spectrum of the biofabricated IONPs (black line) and *S. officinalis* extract (red line). (For interpretation of the references to color in this figure legend, the reader is referred to the web version of this article.)

(Fig. 2b).

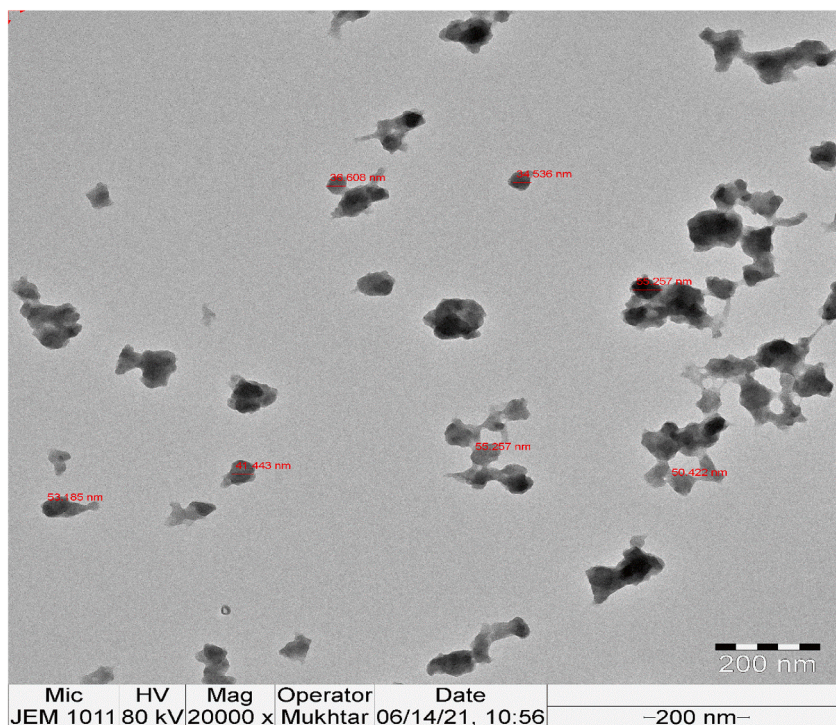
3.4. EDX analysis of biogenic IONPs

The elemental analysis of the phyto-synthesized IONPs was distinguished using EDX analysis. In this context, the characteristic signals of Fe were actually detected at 0.8, 6.4 and 7.0 keV for Fe L_{α} , Fe K_{α} and Fe K_{β} , whereas the signals of C and O were detected at 0.3 and 0.5 keV, respectively (Fig. 3). Moreover, the prominent peak of silicon was detected at 1.7 keV, which could be allotted to the capping molecules of *S. officinalis* utilized in the synthesis procedure. The carbon peak was accredited to the carbon tape that was used for positioning the biogenic IONPs on the sample holder. Accordingly, the mass percentage (%) of Fe in IONPs was recalculated and the detected mass % was detected to be 56.46 % after excluding the mass % of C element.

3.5. FTIR analysis of the phyto-synthesized IONPs

Fourier-transform infrared spectroscopy analysis was conducted to determine the main functional groups of the phyto-synthesized IONPs. FTIR spectra of the biologically synthesized IONPs exhibited the existence of six absorption peaks at the following wavenumbers: 3434.75, 1627.30, 1384.17, 1261.97, 1048.24, and 586.21 cm^{-1} , correspondingly. (Fig. 4). The broad band detected at 3434.75 cm^{-1} could be assigned to O-H stretching of phenolic compounds whereas the peak noticed at 1627.30 cm^{-1} might be attributed to C = C stretching vibrations of aromatic compounds as flavonoids and polyphenolic compounds. Additionally, it is worth noting that the band detected at a

A



B

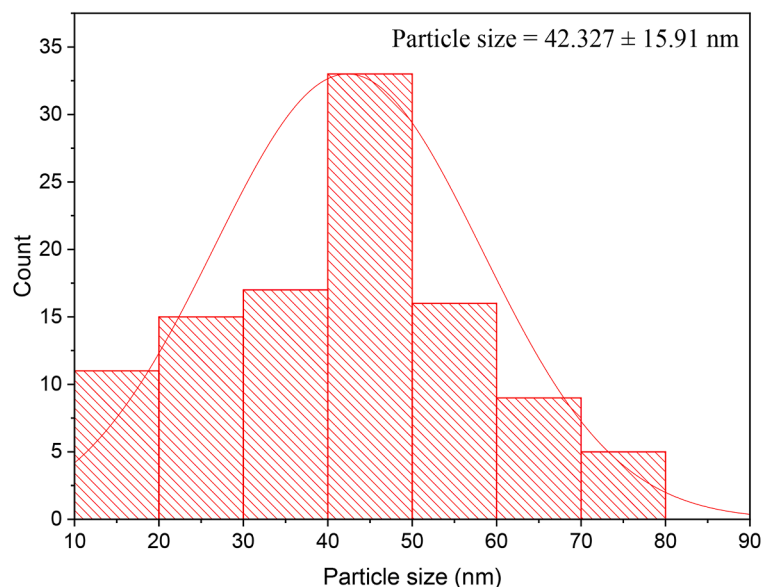


Fig. 2. (A) TEM micrograph of the biosynthesized IONPs, (B) Particle size distribution of the biogenic IONPs.

wavenumber of 1384.17 cm^{-1} may be attributed to the stretching vibrations of C–H bonds in aldehydes. Similarly, the peaks observed at 1261.97 cm^{-1} can be attributed to the stretching vibrations of C–N bonds in aromatic amines. Likewise, the band seen at a wavenumber of 1048.24 cm^{-1} may be attributed to the stretching vibration of the carbon–nitrogen bond in amines. The broadband seen at a wavenumber of 586.21 cm^{-1} may be attributed to the Fe–O stretching vibration in hematite (Fe_2O_3).

3.6. XRD analysis of the biosynthesized IONPs

XRD analysis affirmed the formation of nine distinct diffraction

peaks at 2 theta degrees of 24.80° , 33.41° , 35.03° , 41.28° , 49.15° , 53.41° , 57.37° , 62.40° and 64.31° , assigned to the lattice planes of (012), (104), (110), (202), (024), (116), (211), (214) and (300), respectively (Fig. 5).

3.7. Zeta potential and zetasizer analysis of the phyto-synthesized IONPs

The hydrodynamic diameter of the IONPs synthesized using *S. officinalis* leaves was detected to be 681.4 nm (Fig. 6A), which was notably higher than the diameter measured by transmission electron microscopy (TEM). The biogenic IONPs surface charge was found to be -5.48 mV (Fig. 6B).

JED-2200 Series

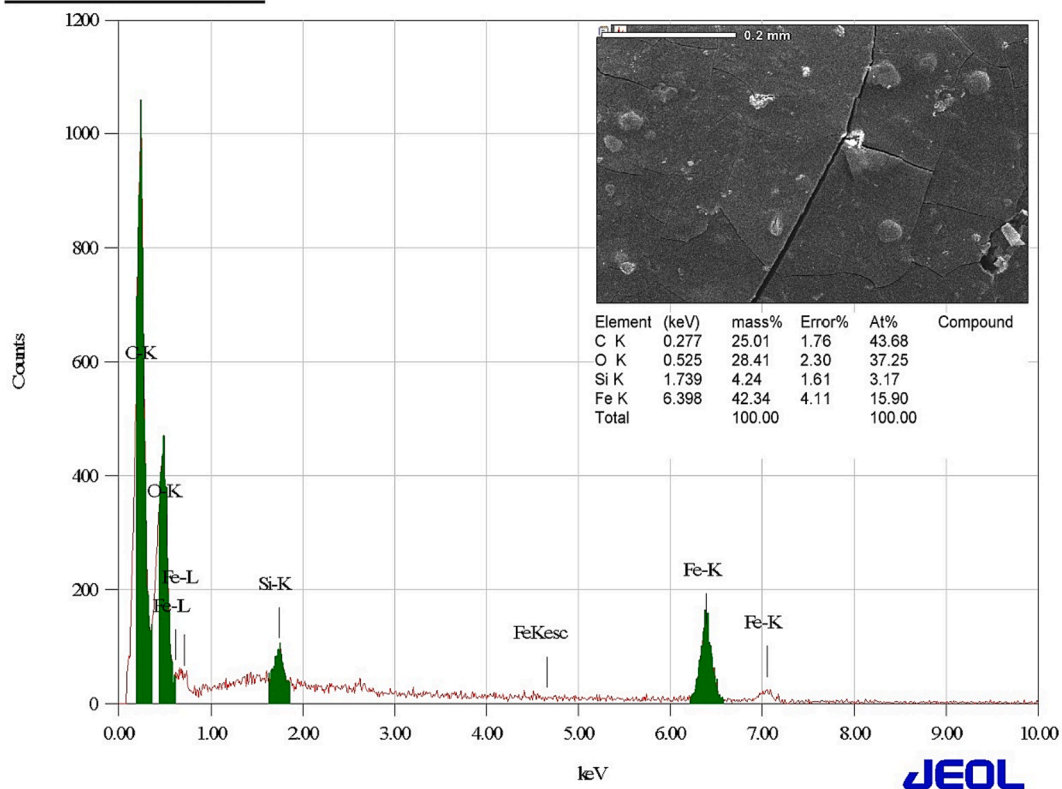


Fig. 3. Elemental composition of the biofabricated IONPs.

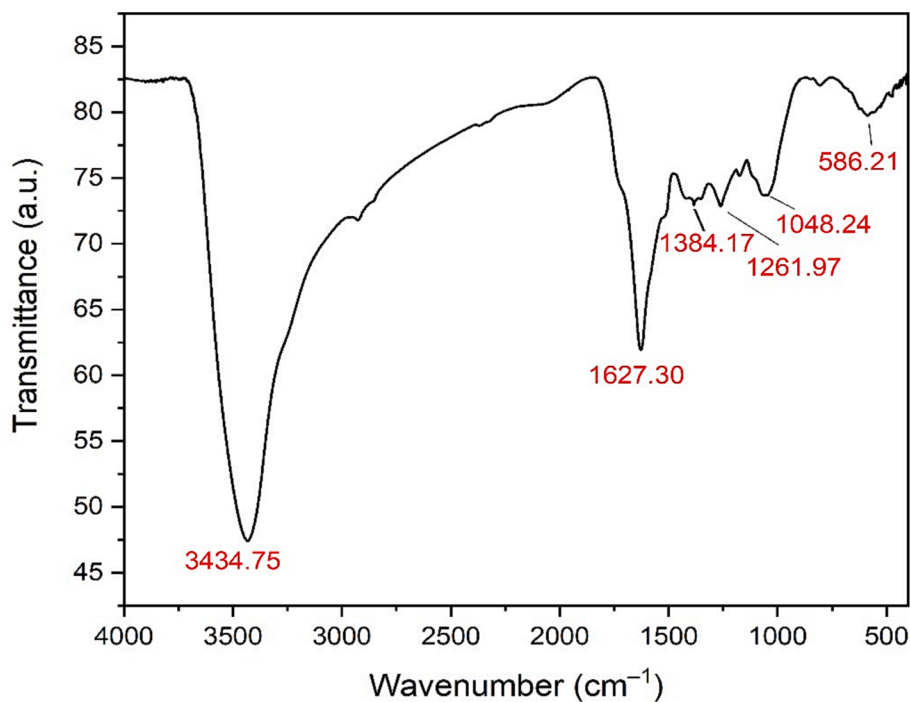


Fig. 4. FTIR spectrum of the biosynthesized IONPs.

3.8. Antibacterial effectiveness of the phyto-synthesized IONPs

The antibacterial effectiveness of the greenly synthesized IONPs was evaluated against *E. coli*, *P. aeruginosa* and MRSA strains using the disk

diffusion method (Fig. 7). In this setting, the biogenic IONPs (200 µg/disk) synthesized using *S. officinalis* extract revealed antibacterial efficiency against *E. coli* and *P. aeruginosa* strains demonstrating relative inhibitory zones of 21.14 ± 0.16 and 17.26 ± 0.26 mm, respectively

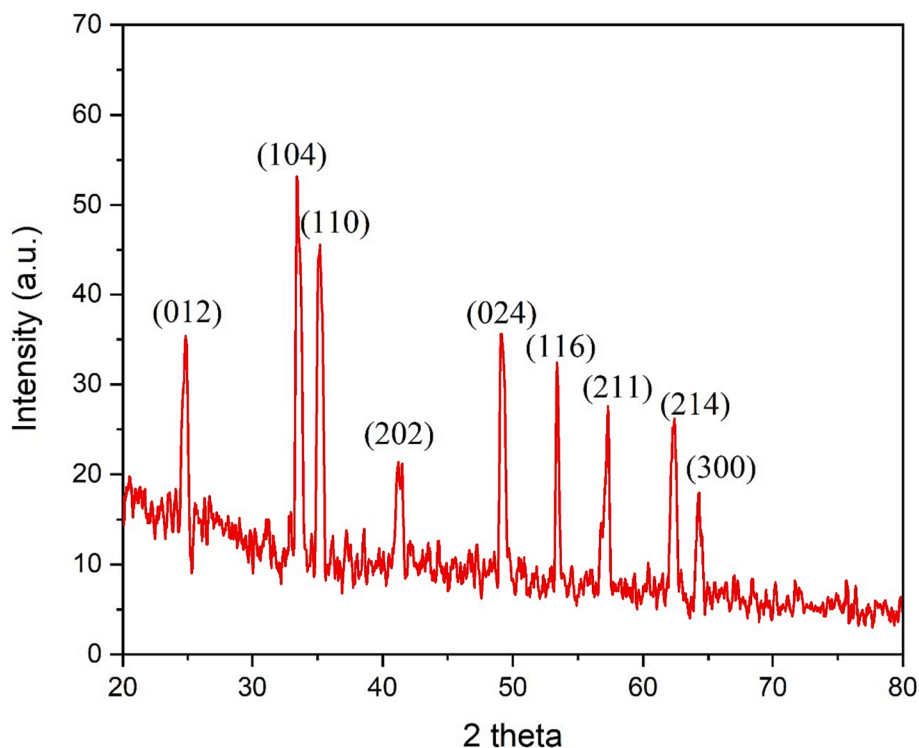


Fig. 5. XRD pattern of the biogenic IONPs.

(Table 1). Moreover, the biogenic IONPs revealed antibacterial efficiency against the tested MRSA strain recording relative inhibitory zone of 9.17 ± 0.48 , 20.56 ± 0.62 mm, respectively. However, faint inhibitory zones were detected at $100 \mu\text{g}/\text{disk}$ against bacterial pathogens. The minimum inhibitory concentration of the phyto-synthesized IONPs was detected to be $80 \mu\text{g}/\text{ml}$ against *E. coli* strain whereas the minimum bactericidal concentration was detected to be $160 \mu\text{g}/\text{ml}$.

3.9. Synergistic antibacterial effectiveness of biogenic IONPs with tigecycline

The synergistic antibacterial efficiency of the biogenic IONPs ($200 \mu\text{g}/\text{disk}$) with tigecycline antibiotic was estimated using disk diffusion method. In this context, the highest synergistic percentage of tigecycline + IONPs combination was detected against 67.15 % against *E. coli* strain whereas the lowest synergistic percentage was detected against *P. aeruginosa* strain, with relative percentage of 38.85 %. Moreover, the tigecycline + IONPs combination exposed a synergistic antibacterial efficiency against MRSA strain with relative synergism percentage of 51.6 % (Table 2).

4. Discussion

The *S. officinalis* water extract has been found to be a key factor in green fabrication of IONPs, a type of iron nanoparticles. The extract, rich in bioactive constituents such as phenolic compounds, saponins, tannins, alkaloids, flavonoids, glucosides, steroids, and proteins, has been shown to have antibacterial properties against various bacterial pathogens (Ghorbani and Esmailizadeh, 2017). The antibacterial efficacy of the bioformulated IONPs may be due to the capping molecules of the biogenic IONPs, as demonstrated by FTIR analysis (Sulaiman et al., 2023). The water extract serves as a reducing agent for ferric nitrate solutions, aiding in the formation of IONPs, and as a stabilizing agent, preventing the agglomeration of synthesized nanoparticles (Sidhu et al., 2022).

The reduction of metal ions is influenced by the surface chemistry of

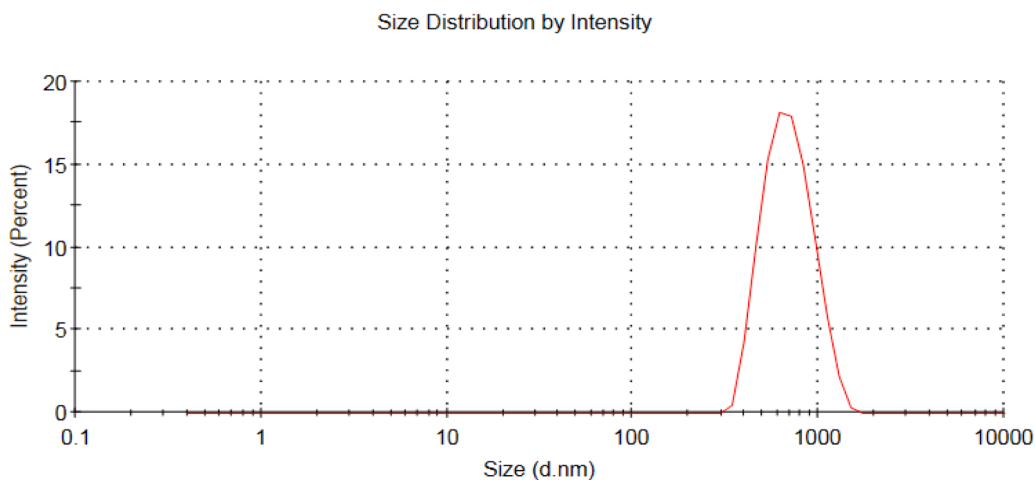
reducing agents, including functional groups like $-\text{C}=\text{C}$, $-\text{OH}$, $-\text{C}-\text{N}$, and $-\text{C}-\text{H}$. Bioreduction consists of four stages: activation phase, nucleation phase, growth phase, and termination phase. The activation phase involves the gradual formation of nanoparticles, facilitated by biomolecules in the extract. The nucleation phase involves crystal development on metal nuclei while being reduced by biometabolites. Reducing substances adsorb onto the surface of metal nanoparticles act as chelating and capping agents. The subsequent development phase transitions metal ions to zero valence oxidation states. The development progression stage involves metallic nanoparticles aggregating to achieve various morphologies. In the termination phase, nanoparticles reach their final stable shape and are coated with biomolecules, increasing steric repulsion, which is believed to mitigate agglomeration issues (Priya et al., 2021). The study focused on the green biosynthesis of IONPs using *S. officinalis* leaf extract, which has been found to be highly efficient. The absorption peak at 349 nm was assigned to the biogenic IONPs, and this finding was consistent with previous investigations (Devi et al., 2021). XRD data confirmed the rhombohedral crystalline structure of the phyto-synthesized IONPs, which corresponds to the crystalline configuration of Fe_2O_3 (Muthukumar and Matheswaran, 2015). Iron oxide crystals with a rhombohedral structure have the highest degree of stability, with Fe^{3+} ions occupying two-thirds of the octahedral positions contained by an almost perfect hexagonal close-packed Oxygen lattice (Busti et al., 2021).

Dynamic light scattering revealed that the average particle size was higher than that of TEM analysis, which can be attributed to the fact that DLS accounts for both the hydrodynamic size, encompassing both the core size and shell thickness, whereas TEM analysis solely captures the core of the IONPs (Arsalani et al., 2018). The negative charge of the biogenic IONPs was detected to be -5.48 mV, which signifies that the biogenic IONPs possess the ability to repel one another, providing enhanced colloidal stability. Numerous factors contribute to the stability of nanoparticles, such as the physicochemical characteristics of the solvent and extract, electrostatic interactions, and van der Waals forces. The significance of incorporating hydroxyl (OH) functional groups onto the surface of the biogenic IONPs was shown to be essential in the

A

	Size (d.nm):	% Intensity:	St Dev (d.n...)
Z-Average (d.nm): 681.4	Peak 1: 707.1	100.0	211.4
Pdl: 0.155	Peak 2: 0.000	0.0	0.000
Intercept: 0.893	Peak 3: 0.000	0.0	0.000

Result quality : Good



B

	Mean (mV)	Area (%)	St Dev (mV)
Zeta Potential (mV): -5.48	Peak 1: -5.48	100.0	3.66
Zeta Deviation (mV): 3.66	Peak 2: 0.00	0.0	0.00
Conductivity (mS/cm): 0.0690	Peak 3: 0.00	0.0	0.00

Result quality : Good

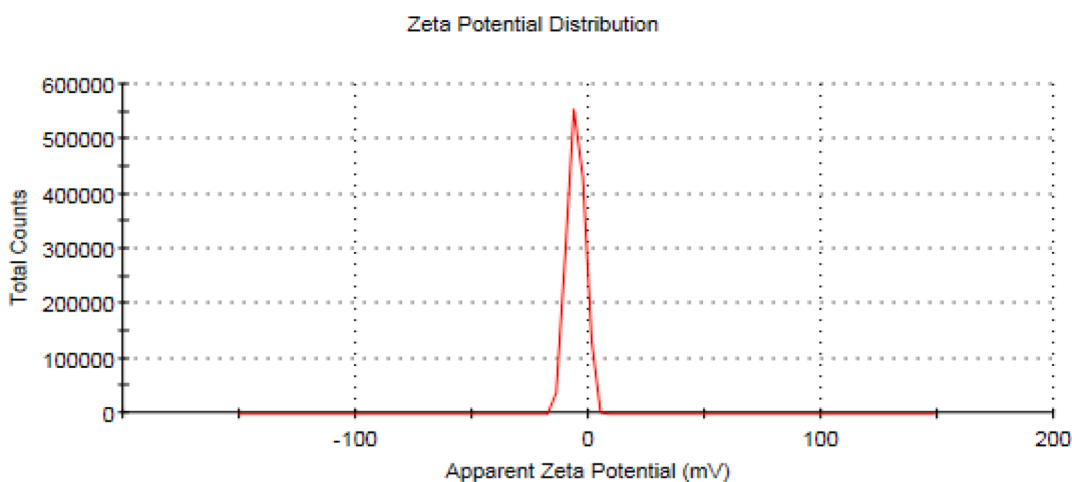


Fig. 6. (A) The hydrodynamic diameter of the biogenic IONPs, (B) Zeta potential of the biofabricated IONPs.

production of negative charges on the nanoparticles. TEM micrographs of phyto-synthesized IONPs revealed a matrix-like structure, which could be assigned to the capping molecules. The Fe element had a detected mass percentage of 42.3 %, indicating a slight increase compared to the findings of a prior investigation (Ansari and Asiri, 2021). The phyto-synthesized IONPs (200 µg/disk) of *S. officinalis* extract revealed antibacterial activity against *E. coli*, MRSA, and *P. aeruginosa* strains with inhibitory zones ranging from 17.26 ± 0.26 to

21.14 ± 0.16 mm in diameter, respectively. In this setting, the antibacterial activity was significantly higher than that of a prior study which indicated that the biogenic IONPs synthesized using *Lagenaria siceraria* at the concentration of 20 mg/ml exhibited antibacterial efficiency against *E. coli* strain with inhibitory zones of 10 mm in diameter (Kanagasubbulakshmi and Kadirvelu, 2017). The difference in the antibacterial efficacy of the greenly synthesized IONPs as reported in different studies could be attributed to the use of different biological

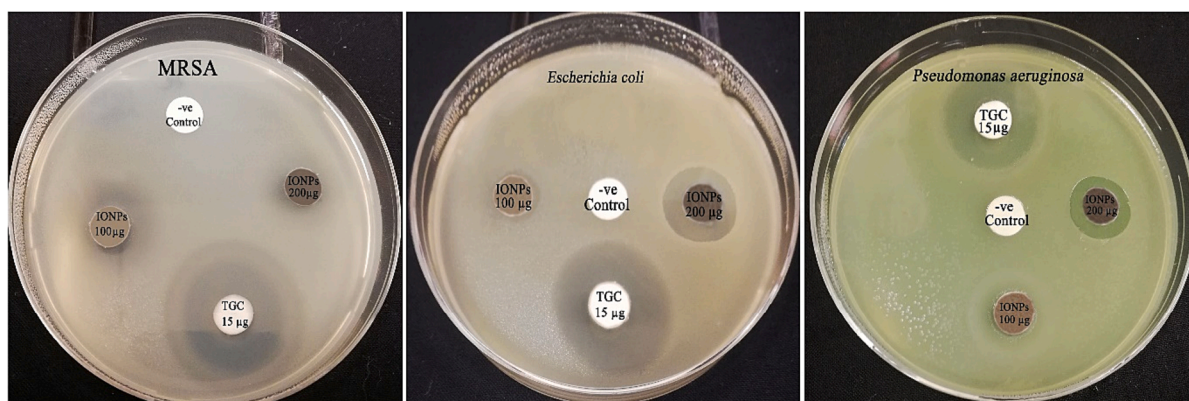


Fig. 7. Antimicrobial activity of the phyto-synthesized IONPs (IONPs) against *E. coli* and *P. aeruginosa* strains.

Table 1

Antibacterial efficiency of biogenic IONPs (IONPs) against the tested bacterial pathogens.

Bacterial strains	IONPs (100 µg/disk)	IONPs (200 µg/disk)	Tigecycline (15 µg/disk)	Negative control
MRSA	9.17 ± 0.48	20.56 ± 0.62	22.41 ± 0.75	0.00 ± 0.00
<i>E. coli</i>	8.78 ± 0.53	21.14 ± 0.16	23.09 ± 0.56	0.00 ± 0.00
<i>P. aeruginosa</i>	10.59 ± 0.38	17.26 ± 0.26	19.81 ± 0.64	0.00 ± 0.00

Table 2

Synergistic antibacterial efficiency of biogenic IONPs (IONPs) with tigecycline against the tested bacterial pathogens.

Bacterial strains	Tigecycline (15 µg/disk)	IONPs (200 µg/disk)	Tigecycline (15 µg/disk) + IONPs (200 µg/disk)	Synergism %	IFA
MRSA	21.51 ± 0.61	19.74 ± 0.31	32.61 ± 0.85	51.60 %	1.29
<i>E. coli</i>	22.65 ± 0.48	21.38 ± 0.76	37.86 ± 0.38	67.15 %	1.79
<i>P. aeruginosa</i>	19.74 ± 0.52	17.51 ± 0.43	27.41 ± 0.11	38.85 %	0.93

*IFA: increase in fold of inhibition area.

agents during the synthesis process. This, in turn, influences the size of the biosynthesized IONPs and also the capping molecules present on their surface, both of which collectively impact their antibacterial efficiency. The antibacterial properties of IONPs are believed to be influenced by factors such as the oxide form, morphology, size, and other physicochemical properties of the nanoparticles.

Reactive oxygen species generation is a significant mechanism of toxicity in IONPs, as evidenced previously (Zakariya et al., 2022). In this context, ROS exhibit genotoxic properties by causing damage to DNA molecules. A decrease in the activity of antioxidant system enzymes has been identified as a potential cause for the observed increase in ROS concentration. Metal ions have the capability to form bonds with thiol (-SH), amino (-NH), and carboxyl (-COOH) functional groups present in proteins, such as enzymes. This interaction can result in the inactivation or partial inhibition of these proteins (Rana et al., 2023).

The combination of tigecycline and IONPs demonstrated a synergistic effect in terms of antibacterial activity against the tested strains. The findings of this study indicate that the biogenic IONPs, at a concentration of 500 µg/ml, exhibited enhanced antibacterial activity

against the tested strains. The combined action of IONPs (IONPs) with tetracycline resulted in larger inhibitory zones, measuring 19, 20, and 28 mm, compared to the inhibitory zones observed when using tetracycline alone, which measured 0, 12, and 15 mm, respectively. The biogenic IONPs derived from the extract of *S. officinalis* exhibited a notable synergistic effect with tigecycline when tested at a concentration approximately half that of the previous study (Ahmed et al., 2021). The potential mechanism underlying the synergistic effects observed when combining IONPs with antibiotics could be attributed to the positive charges exhibited by the metal nanoparticles and the negative charges possessed by microorganisms. This electrostatic attraction between the nanoparticles and microorganisms' likely leads to the oxidation of the microorganisms. Furthermore, the nanoparticles release ions that interact with the thiol groups (-SH) found on the surface proteins of bacterial cells, ultimately resulting in cell lysis. The concurrent action of IONPs and antibiotics exhibits a synergistic effect, facilitating the efficient infiltration of antibiotics into bacterial cells owing to the tiny size of the biogenic nanoparticles, ultimately leading to bacterial lysis (Patra and Baek, 2017).

5. Conclusion

The green production of biogenic IONPs, with potential antibacterial properties, was achieved using the aqueous leaf extract of *S. officinalis*. The spherical nanoparticles, with an average size of 42.3 nm and a surface charge of -5.48 mV, have antimicrobial activity against nosocomial bacterial pathogens. These nanoparticles could be used in the production of disinfectants for surfaces in hospitals and healthcare settings. The synergistic efficiency of the biogenic IONPs in combination with tigecycline antibiotics could reduce antibiotic use, potentially decreasing multi-drug resistant pathogens, and improving control of nosocomial infections in healthcare facilities.

CRedit authorship contribution statement

Mohamed Taha Yassin: Conceptualization, Funding acquisition, Writing – original draft, Writing – review & editing. **Fatimah O. Al-Otibi:** Methodology, visualization, validation, software. **Abdulaziz A. Al-Askar:** Supervision, resources, and project administration.

Declaration of competing interest

The authors declare that they have no known competing financial interests or personal relationships that could have appeared to influence the work reported in this paper.

Acknowledgments

The authors extend their appreciation to the Researchers Supporting Project number (RSPD2024R1105), King Saud University, Riyadh, Saudi Arabia.

Appendix A. Supplementary material

Supplementary data to this article can be found online at <https://doi.org/10.1016/j.jksus.2024.103131>.

References

- Ahmed, B., Syed, A., Ali, K., M. Elgorban, A., Khan, A., Lee, J., A. Al-Shwaiman, H., 2021. Synthesis of gallotannin capped iron oxide nanoparticles and their broad spectrum biological applications. *RSC Adv.* 11, 9880–9893. <https://doi.org/10.1039/D1RA00220A>.
- Akintelu, S.A., Oyebamiji, A.K., Olugbeko, S.C., Folorunso, A.S., 2021. Green synthesis of iron oxide nanoparticles for biomedical application and environmental remediation: a review. *Eclética Química* 46 (4), 17–37.
- Al-Otibi, F.O., Yassin, M.T., Al-Askar, A.A., Maniah, K., 2023. Green biofabrication of silver nanoparticles of potential synergistic activity with antibacterial and antifungal agents against some nosocomial pathogens. *Microorganisms* 11, 945. <https://doi.org/10.3390/microorganisms11040945>.
- Arakiyaraaj, S., Saravanan, M., Udaya Prakash, N.K., Valan Arasu, M., Vijayakumar, B., Vincent, S., 2013. Enhanced antibacterial activity of iron oxide magnetic nanoparticles treated with Argemone mexicana L. leaf extract: An in vitro study. *Mater. Res. Bull.* 48, 3323–3327. <https://doi.org/10.1016/j.materresbull.2013.05.059>.
- Arsalani, S., Guidelli, E.J., Araujo, J.F.D.F., Bruno, A.C., Baffa, O., 2018. Green synthesis and surface modification of iron oxide nanoparticles with enhanced magnetization using natural rubber latex. *ACS Sustain. Chem. Eng.* 6, 13756–13765. <https://doi.org/10.1021/acssuschemeng.8b01689>.
- Busti, N.D., Parra, R., Sousa Góes, M., 2021. Synthesis, Properties, and Applications of Iron Oxides: Versatility and Challenges. In: La Porta, F.A., Taft, C.A. (Eds.), *Functional Properties of Advanced Engineering Materials and Biomolecules, Engineering Materials*. Springer International Publishing, Cham, pp. 349–385. https://doi.org/10.1007/978-3-030-62226-8_13.
- De Oliveira, D.M.P., Forde, B.M., Kidd, T.J., Harris, P.N.A., Schembri, M.A., Beatson, S. A., Paterson, D.L., Walker, M.J., 2020. Antibiotic resistance in ESKAPE pathogens. *Clin. Microbiol. Rev.* 33, e00181–e219. <https://doi.org/10.1128/CMR.00181-19>.
- Duan, H., Wang, D., Li, Y., 2015. Green chemistry for nanoparticle synthesis. *Chem. Soc. Rev.* 44, 5778–5792. <https://doi.org/10.1039/C4CS00363B>.
- Ghorbani, A., Esmaeilzadeh, M., 2017. Pharmacological properties of Salvia officinalis and its components. *J. Tradit. Complement. Med.* 7, 433–440. <https://doi.org/10.1016/j.jtcme.2016.12.014>.
- Groiss, S., Selvaraj, R., Varadavenkatesan, T., Vinayagam, R., 2017. Structural characterization, antibacterial and catalytic effect of iron oxide nanoparticles synthesised using the leaf extract of Cynometra ramiflora. *J. Mol. Struct.* 1128, 572–578. <https://doi.org/10.1016/j.molstruc.2016.09.031>.
- Hetta, H.F., Ramadan, Y.N., Al-Harbi, A.I., Ahmed, E., Battah, B., Abd Ellah, N.H., Zanetti, S., Donadu, M.G., 2023. Nanotechnology as a Promising Approach to Combat Multidrug Resistant Bacteria: A Comprehensive Review and Future Perspectives. *Biomedicine* 11, 413. <https://doi.org/10.3390/biomedicine11020413>.
- Kaasch, A.J., Barlow, G., Edgeworth, J.D., Fowler Jr, V.G., Hellmich, M., Hopkins, S., Kern, W.V., Llewelyn, M.J., Rieg, S., Rodriguez-Baño, J., 2014. Staphylococcus aureus bloodstream infection: a pooled analysis of five prospective, observational studies. *J. Infect.* 68, 242–251.
- Kanagasubbulakshmi, S., Kadirvelu, K., 2017. Green synthesis of Iron oxide nanoparticles using Lagenaria siceraria and evaluation of its antimicrobial activity. *Def. Life Sci. J.* 2, 422. <https://doi.org/10.14429/dlsj.2.12277>.
- Mills, E.G., Martin, M.J., Luo, T.L., Ong, A.C., Maybank, R., Corey, B.W., Harless, C., Preston, L.N., Rosado-Mendez, J.A., Preston, S.B., Kwak, Y.L., Backlund, M.G., Bennett, J.W., Mc Gann, P.T., Lebreton, F., 2022. A one-year genomic investigation of Escherichia coli epidemiology and nosocomial spread at a large US healthcare network. *Genome Med.* 14, 147. <https://doi.org/10.1186/s13073-022-01150-7>.
- Muthukumar, H., Matheswaran, M., 2015. Amaranthus spinosus leaf extract mediated FeO nanoparticles: physicochemical traits, photocatalytic and antioxidant activity. *ACS Sustain. Chem. Eng.* 3, 3149–3156.
- Pallela, P.N.V.K., Ummey, S., Ruddaraju, L.K., Gadi, S., Cherukuri, C.S., Barla, S., Pammi, S.V.N., 2019. Antibacterial efficacy of green synthesized α -Fe₂O₃ nanoparticles using Sida cordifolia plant extract. *Heliyon* 5, e02765. <https://doi.org/10.1016/j.heliyon.2019.e02765>.
- Patra, J.K., Ali, M.S., Oh, I.-G., Baek, K.-H., 2017. Proteasome inhibitory, antioxidant, and synergistic antibacterial and anticandidal activity of green biosynthesized magnetic Fe₃O₄ nanoparticles using the aqueous extract of corn (Zea mays L.) ear leaves. *Artif. Cells Nanomed. Biotechnol.* 45, 349–356. <https://doi.org/10.3109/21691401.2016.1153484>.
- Patra, J.K., Baek, K.-H., 2017. Green biosynthesis of magnetic iron oxide (Fe₃O₄) nanoparticles using the aqueous extracts of food processing wastes under photocatalyzed condition and investigation of their antimicrobial and antioxidant activity. *J. Photochem. Photobiol. B* 173, 291–300. <https://doi.org/10.1016/j.jphotobiol.2017.05.045>.
- Priya, N., Kaur, K., Sidhu, A.K., 2021. Green synthesis: An eco-friendly route for the synthesis of iron oxide nanoparticles. *Front. Nanotechnol.* 3, 655062.
- Rana, A., Pathak, S., Lim, D.-K., Kim, S.-K., Srivastava, R., Sharma, S.N., Verma, R., 2023. Recent advancements in plant- and microbe-mediated synthesis of metal and metal oxide nanomaterials and their emerging antimicrobial applications. *ACS Appl. Nano Mater.* 6, 8106–8134. <https://doi.org/10.1021/acsnm.3c01351>.
- Sajid, M., Plotka-Wasylyk, J., 2020. Nanoparticles: Synthesis, characteristics, and applications in analytical and other sciences. *Microchem. J.* 154, 104623. <https://doi.org/10.1016/j.microc.2020.104623>.
- Sathishkumar, G., Logeshwaran, V., Sarathbabu, S., Jha, P.K., Jeyaraj, M., Rajkuberan, C., Senthilkumar, N., Sivaramakrishnan, S., 2018. Green synthesis of magnetic Fe₃O₄ nanoparticles using Couroupita guianensis Aubl. fruit extract for their antibacterial and cytotoxicity activities. *Artif. Cells Nanomed. Biotechnol.* 46, 589–598. <https://doi.org/10.1080/21691401.2017.1332635>.
- Shkodenko, L., Kassirov, I., Koshel, E., 2020. Metal oxide nanoparticles against bacterial biofilms: Perspectives and limitations. *Microorganisms* 8, 1545. <https://doi.org/10.3390/microorganisms8101545>.
- Sidhu, A.K., Verma, N., Kaushal, P., 2022. Role of Biogenic Capping Agents in the Synthesis of Metallic Nanoparticles and Evaluation of Their Therapeutic Potential. *Front. Nanotechnol.* 3.
- Sulaiman, A.M., Abdulaziz, A.S., Almutawea, A.M., Alansari, S.A., Aldoseri, F.A., Bekhit, S.A., Althawadi, S.M., Alqallaf, S.M., Bekhit, A.A., 2023. Evaluation of the antibacterial effect of salvia officinalis essential oil and its synergistic effect with Meropenem. *Lett. Appl. Nanobiosci.* 12, 44.
- Yassin, M.T., Mostafa, A.A.F., Al-Askar, A.A., Alkhelaif, A.S., 2022. In vitro antimicrobial potency of Elettaria cardamomum ethanolic extract against multidrug resistant of food poisoning bacterial strains. *J. King Saud Univ. Sci.* 34 (6), 102167.
- Zakariya, N.A., Majeed, S., Jusof, W.H.W., 2022. Investigation of antioxidant and antibacterial activity of iron oxide nanoparticles (IONPS) synthesized from the aqueous extract of Penicillium spp. *Sens. Int.* 3, 100164. <https://doi.org/10.1016/j.sintl.2022.100164>.